Article:
Macháčková, Kateřina, Collinsová, Michaela, Chrudinová, Martina et al. (7 more authors) (2017) Insulin-like Growth Factor 1 Analogs Clicked in the C Domain:Chemical Synthesis and Biological Activities. JOURNAL OF MEDICINAL CHEMISTRY. pp. 10105-10117. ISSN: 0022-2623

https://doi.org/10.1021/acs.jmedchem.7b01331

Journal of Medicinal Chemistry

Article

Cite This: J. Med. Chem. 2017, 60, 10105−10117

pubs.acs.org/jmc

Insulin-like Growth Factor 1 Analogs Clicked in the C Domain: Chemical Synthesis and Biological Activities

Kateřina Macháčková,[†] Michaela Collinsová,[†] Martina Chrudinová,[†] Irena Selicharová,[†] Jan Pícha,[†] Miloš Buděšínský,[†] Václav Vaněk,[†] Lenka Žáková,[†] Andrzej M. Brzozowski,[‡] and Jiří Jiráček*[,†]

[†]Institute of Organic Chemistry and Biochemistry, The Czech Academy of Sciences, Flemingovo nám. 2, 166 10 Prague 6, Czech Republic

[‡]York Structural Biology Laboratory, Department of Chemistry, The University of York, Heslington, York YO10 5DD, United Kingdom

Supporting Information

ABSTRACT: Human insulin-like growth factor 1 (IGF-1) is a 70 amino acid protein hormone, with key impact on growth, development, and lifespan. The physiological and clinical importance of IGF-1 prompted challenging chemical and biological trials toward the development of its analogs as molecular tools for the IGF-1 receptor (IGF1-R) studies and as new therapeutics. Here, we report a new method for the total chemical synthesis of IGF-1 analogs, which entails the solid-phase synthesis of two IGF-1 precursor chains that is followed by the Cu^{I}-catalyzed azide−alkyne cycloaddition ligation and by biomimetic formation of a native pattern of disulfides. The connection of the two IGF-1 precursor chains by the triazole-containing moieties, and variation of its neighboring sequences (Arg36 and Arg37), was tolerated in IGF-1R binding and its activation. These new synthetic IGF-1 analogs are unique examples of disulfide bonds' rich proteins with intra main-chain triazole links. The methodology reported here also presents a convenient synthetic platform for the design and production of new analogs of this important human hormone with non-standard protein modifications.

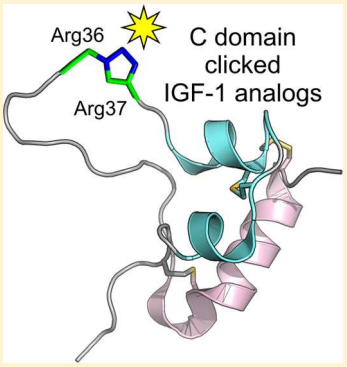

INTRODUCTION

Human insulin and related insulin-like growth factors 1 and 2 (IGF-1 and IGF-2) are small protein hormones, with a key impact on basal metabolism, growth, development,[1−3] lifespan,[4,5] as well as being implicated in diabetes and cancer.[6,7] Hence their central biological importance and involvement in many relevant human pathologies require efforts toward the development of specific analogs of these hormones for studies of the interactions and signaling with respective insulin- and IGF-receptors (IR, IGF-1R) and their applications as new therapeutics.[3−9] The recombinant production of insulin and IGFs in *E. coli*, or in yeast, was an obvious choice,[10−12] but did not easily allow the incorporation of non-coded amino acids and unusual structural motifs, which could facilitate more directed structure−activity studies of the hormones and their rational modifications. Moreover, the total chemical synthesis of these proteins, especially of IGF-1 and -2, remains a very challenging task.[13]

The single-chain organization, fold, and disulfide bond pattern of IGF-1/IGF-2 is similar to proinsulin, a prohormone of insulin, but they are significantly longer (70, 67, and 86 residues, respectively) than both insulin chains (21 and 30 amino acids). Therefore, their solid-phase synthesis is challenging and inefficient as demonstrated by only few early reports on the total chemical synthesis of IGF-1 analogs.[14−16] Nevertheless, elegant studies employed a combination of shorter protein fragments by a native ligation for the synthesis of human proinsulin,[17] single chain "ester" insulin,[18,19] and IGF-1 analog.[20] The complexity of the synthesis of these hormones is highlighted further by only one report on the total chemical synthesis of IGF-2.[21]

Therefore, our aim here was to develop a new methodology for the chemical synthesis of IGF-1 analogs as a feasible alternative for the production of single-chain insulin-like hormones, and one that would allow easy incorporation of non-standard amino acids or other unusual structural motifs.

As the solid-phase synthesis of a single, 70-amino acid chain of IGF-1 is inefficient, in this work we combined the solid-phase synthesis of two shorter precursor IGF-1 fragments with their ligation by a Cu^{I}-catalyzed 1,3-dipolar cycloaddition of azides and alkynes,[22−24] followed by the biomimetic formation of the native pattern of disulfide bridges. Cu^{I}-catalyzed 1,3-dipolar cycloaddition of azides and alkynes is a biorthogonal reaction, also called a "click" chemistry, which leads to the formation of 1,4-disubstituted 1,2,3-triazoles. This reaction has become widely used[25] in organic, medicinal, and, especially, peptide chemistry,[26] as 1,2,3-triazole is a motif with the structural and electronic characteristics similar to those of the peptide bond.[27,28]

The synthesis of insulin and insulin-like proteins is difficult due to the necessity to form three disulfide bridges. Therefore,

Received: September 6, 2017
Published: November 27, 2017

DOI: 10.1021/acs.jmedchem.7b01331
J. Med. Chem. 2017, 60, 10105−10117

a number of sophisticated methods of insulin synthesis have been developed, usually with an orthogonal protection of cysteines (e.g., in refs 29 and 30 and reviewed in ref 31) and a directed, stepwise formation of disulfides. A similar strategy was developed for other proteins from the insulin family, such as relaxins, DILP, INSL peptides,[32−36] and cone snail insulin.[37] An alternative, and straightforward, method for the formation of disulfides starts with the simultaneous deprotection of all six cysteines (from e.g. *S*-sulfonate protected forms) and pairing by a slow air oxidation. This approach takes advantage of the intrinsic biomimetic ability of insulin chains to adopt a natural conformation and a correct coupling of disulfides.[18,38−43] In this study, we used the strategy of biomimetic formation of disulfides for the synthesis of IGF-1 analogs.

The biological functionality aspect of this work was focused on the role and modifications of the IGF-1 C domain, specifically, at its Arg36 and Arg37 sites. The C domain of IGF-1 (residues 30−41, Figure 1) was found to be important for its

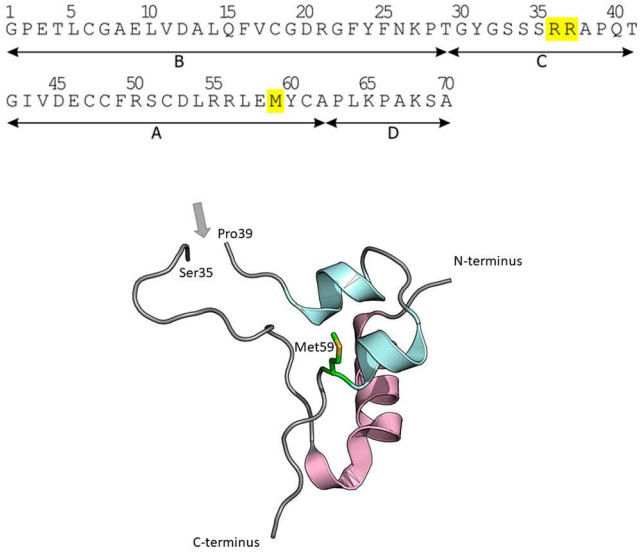

Figure 1. The primary sequence and the 3D fold of human IGF-1. The primary sequence of human IGF-1 (one-letter code, N-terminus is in the left, C-terminus is in the right, upper panel); residues mutated in this study (Arg36, Arg37 and Met59) are highlighted in yellow; disulfide bridges: 47-52, 48-6, and 61-18. The organization of IGF-1 into B, C, A, and D domains is shown below the sequence by arrows, and the 3D fold of its main chain is in the lower panel (1GZR.PDB).[51] The gap in the protein chain (marked by a gray arrow) reflects a typical lack of connectivity between Arg36-Ala38; Met59, mutated in one of the analogs is shown in green, IGF-1 residues 39-66 are in light blue, residues 3-35 are in pink; residues 67-70 and 1-2 were disordered.

functionality,[44−46] as the double Arg36-Arg37 → Ala36-Ala37 mutation severely impaired binding of this mutant to the IGF-1 receptor (IGF-1R)[47] and to IGF binding protein 1 (IGFBP-1), which contributes to the regulation of IGF-1 bioavailability.[48] In addition, a double Arg36-Arg37 → Glu36-Glu37 substitution also indicated a partial antagonism of this analog, that is, its still effective binding to IGF-1R, but an impaired receptor signaling[49] and tumorigenesis.[50]

Interestingly, the connectivity, that is, well-defined electron density for residues Arg36- Arg37-Ala38, and, generally, for this central part of the C domain, was frequently missing in several crystal structures of human free, and IGFBP-bound, IGF-1 (Figure 1).[51−53] It was postulated then that the pair of these basic arginine side chains may constitute an in vivo proteolytic cleavage site. Although the presence of Arg36 and Arg37 in the IGF-1 C domain is important for an efficient binding to IGF-1R,[47] it was not known whether the cleavage of the Arg36-Arg37 peptide bond impairs hormone binding to IGF-1R or if the resulting two-chain IGF-1 is still able to effectively activate IGF-1R. For this reason, we produced a two-chain IGF-1 analog here as well, which is disconnected between sites Arg36 and Arg37.

Together, we designed, synthesized, and characterized one two-chain IGF-1 analog and three single-chain IGF-1 analogs with a connecting triazole bridge between, or in, sites 36 and 37 to probe the feasibility of their synthesis and to test the impact of these modifications on the biological activities of these analogs. In one of the analogs, Met59 was mutated to Nle59 to prevent oxidation of Met. The in vitro functional properties of the analogs were characterized by the determination of their binding affinities to the IGF-1R, insulin receptor isoform A (IR-A), and their receptor-activation potencies. The IR-A receptor was used here as an IR isoform that, in contrast to its IR-B isoform, is a relatively good binder of IGF-1 and, especially, of IGF-2.[12,54,55]

RESULTS

Synthesis. The primary structures of peptide precursors and analogs are shown in Figure 2, and the respective synthetic pathways are overviewed in the Supporting Information Figures S1−S4.

Two-Chain IGF-1 Analog. First, a two-chain human IGF-1 was prepared, referred to as analog **1**, which has a native IGF-1 amino acid sequence, with the same pattern of the disulfide bonds, but it has a split Arg36-Arg37 peptide bond. Hence, analog **1** consists of chain 1-36 and chain 37-70, with all N-termini and C-termini being in the free amine or carboxylic acid forms, respectively (Figure 2).

The individual chains of the analog were prepared by a standard solid-phase synthesis, and the free SH groups of cysteines were converted to *S*-sulfonates (chains **1a** and **1b**, Figure 2) immediately after the cleavage of Trt protecting groups (Figure S1). The chains were recombined (i.e., disulfides formed) to give analog **1** with approximately 0.6% yield (0.2 mg) by a procedure described previously.[42,43]

Single-Chain IGF-1 Analogs. We designed the strategy of the solid-phase peptide synthesis of two shorter IGF-1 chains with *β*-azido-alanine or propargyl glycine at their C- or N-termini, respectively, followed by their ligation by the Cu^{I}-catalyzed azide−alkyne cycloaddition.[22−24] The final synthetic step consisted of the simultaneous biomimetic formation of the native pattern of all three disulfide bridges, as in analog **1**.

The analog **2** was synthesized first (Figures 2 and S2). The synthesis started with the preparation of the chain **2a**, in which the C-terminal Arg36 was replaced by *β*-azido-alanine carboxamide, and the chain **2b**, in which N-terminal Arg37 was replaced by propargyl glycine. Both chains were "clicked", and the single-chain (Acm-protected) precursor **2c** was purified by RP-HPLC. Finally, the Cys-protecting acetamidomethyl (Acm) groups were cleaved, and the analog **2** was allowed to fold by air-induced oxidation.

Next, we synthesized the similar analog **3** from the chains **2a**, **3a**, and **3b** (Figures 2 and S3). The only difference between analogs **2** and **3** was that Met59 was substituted in **3** for norleucine (Nle) to prevent the observed oxidation of Met59

DOI: 10.1021/acs.jmedchem.7b01331
J. Med. Chem. 2017, 60, 10105−10117

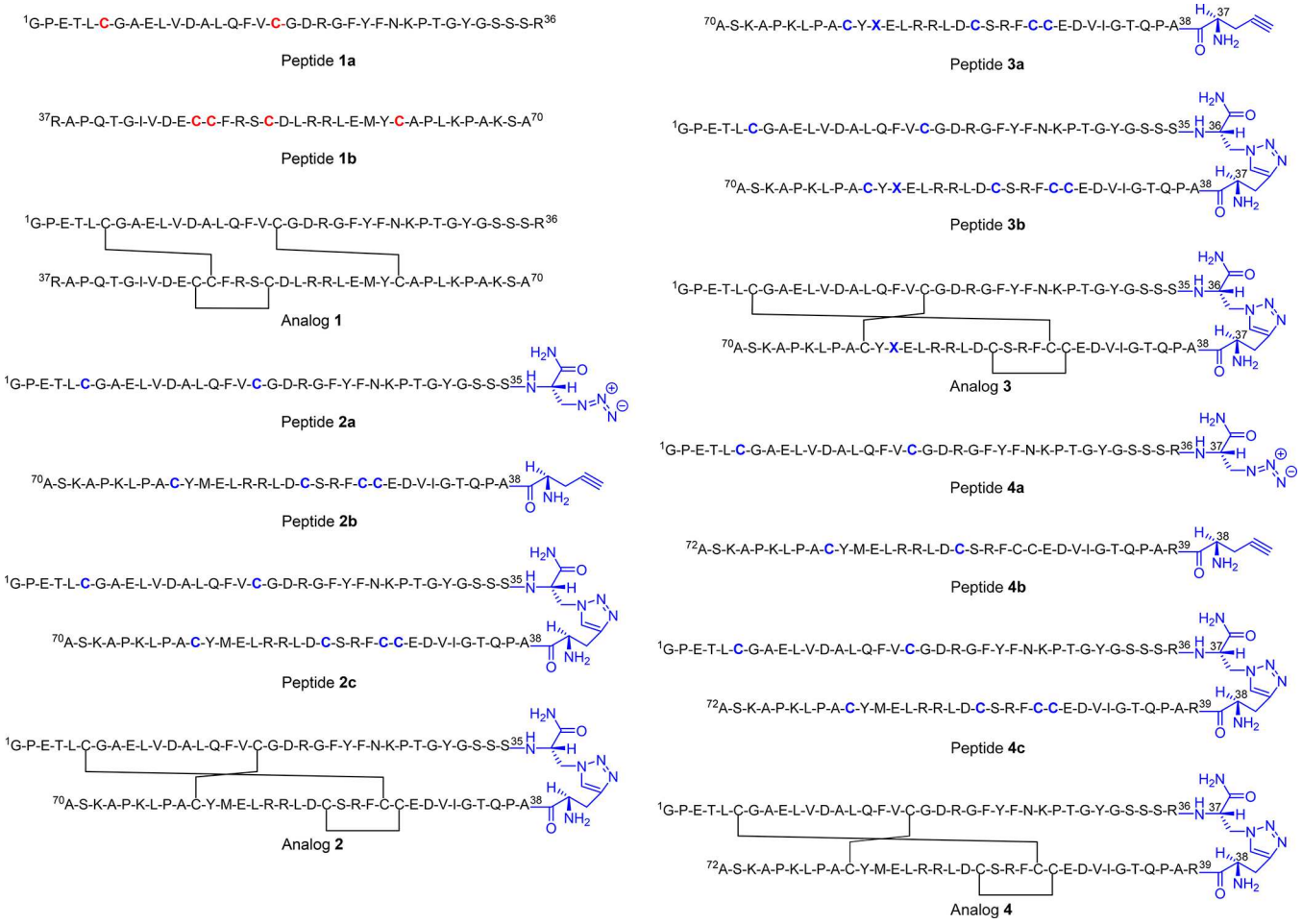

Figure 2. Primary structures of peptide precursors and analogs synthesized in this work. Amino acids are shown in one-letter code. The connecting lines between Cys residues represent disulfide bridges. Unnatural structural features in peptides are highlighted in red or in blue. Red C in peptides **1a** and **1b** represents Cys residues protected by *S*-sulfonate groups. Blue C in peptides **2a**, **2b**, **2c**, **3a**, **3b**, **4a**, **4b**, and **4c** represents Cys residues protected by Acm groups. Blue X in peptides **3a**, **3b**, and analog **3** is norleucine. Azido or propargyl amino acids in **2a**, **2b**, **3a**, **4a**, and **4b** and connecting triazole-containing moieties and **2c**, **2**, **3b**, **3**, **4c**, and **4** are shown in blue as well. ^{1}G and ^{37}R in peptides **1a**, **1b**, and analog **1** are N-terminal residues, and R^{36} and A^{70} in the same peptides are C-terminal residues. ^{1}G is N-terminal glycine in peptides **2a**, **2c**, **3b**, **4a**, **4c**, and analogs **2**−**4**. ^{70}A is C-terminal alanine in peptides **2b**, **2c**, **3b**, **3c**, and analogs **2** and **3**. ^{72}A is C-terminal alanine in peptides **4b**, **4c**, and analog **4**. All terminals of peptides and analogs are in the free forms.

side chain. Finally, we designed and made analog **4** (from the chains **4a**, **4b**, and **4c**, Figures 2 and S4), in which Arg36 was preserved, the triazole link was formed between sites 37−38, with an additional Arg at the position 39; these modifications resulted in an analog that is two amino acids longer than native IGF-1.

In general, the chains with propargyl glycine at the N-terminus (**2b**, **3a**, and **4b**) gave better yields (15−18%) than the azido chains **2a** and **4a** (6−13%). The preparation of the precursor **2a** was hampered by the formation of some byproducts, which were identified as aspartimides (racemized) at positions Asp20 and Arg21 (see analyses and model experiments described in Supporting Information). This problem was largely solved by the use of Fmoc-Asp(OEpe) instead of Fmoc-Asp(O*t*Bu), and the yield improved from 6% to 10%, respectively. We also observed the generation of a byproduct during the synthesis of the peptide **2b**, due to the oxidation of Met59 to methionine sulfoxide. This prompted synthesis of analog **3**, for which the chain **3a** with Met59Nle mutation was used.[27] Although this resulted in a better purity of the crude product **3a**, the yields of HPLC purified peptides **2b** and **3a** were similar (18% and 15%, respectively). Therefore, the native Met59 was retained in peptide **4b**, with only a marginal oxidation of the final product.

Our first attempts (Figure S1) at the click ligation of the azido and alkyne precursor chains were performed as described previously,[42,43] with cysteines protected as *S*-sulfonates. However, we have not succeeded to isolate the desired products here: None of the reaction conditions used (CuBr/TBTA/DIPEA, CuBr/THPTA/DIPEA, CuI/DIPEA, $CuSO_4$/ascorbic acid/THPTA, or $CuSO_4$/ascorbic acid in different organic or aqueous solvents with or without chaotropic agents) was successful, that is, compatible with the use of *S*-sulfonates.

Therefore, the strategy for an efficient disulfide pairing was changed, and all subsequent precursor peptides were synthesized with cysteines protected with Acm groups. Different conditions for the click reactions were investigated, but the only effective setup consisted of an excess of $CuSO_4$/ascorbic acid in *t*BuOH/water, and this methodology[56,57] was employed for the preparation of peptide chains **2c**, **3b**, and **4c**. The effect of different molar ratios of chain precursors for the synthesis of **2c** and **4c** was also tested, and it was observed that

DOI: 10.1021/acs.jmedchem.7b01331
J. Med. Chem. 2017, 60, 10105−10117

Table 1. The Receptor-Binding Affinities of Analogs 1−4 Reported in This Work[a]

Analog	K_d ± SD [nM] (n) for human IGF-1R in mouse fibroblasts	Relative binding affinity for human IGF-1R [%]	K_d ± SD [nM] (n) for human IR-A in IM-9 lymphocytes	Relative binding affinity for human IR-A [%]
Human IGF-1	0.24 ± 0.10 (5)[b]	100 ± 42	23.8 ± 11.5 (3)[c,d]	1.0 ± 0.5
	0.24 ± 0.12 (5)	100 ± 50		
	0.12 ± 0.01 (5)	100 ± 8.3		
Human insulin	291.8 ± 54.3 (3)[b,e]	0.08 ± 0.01	0.24 ± 0.05 (5)[c]	100 ± 21
			0.20 ± 0.04 (5)	100 ± 20
			0.12 ± 0.04 (3)	100 ± 33
			0.32 ± 0.09 (4)	100 ± 28
1	6.74 ± 2.62 (3)[e]	3.56 ± 1.38**	48.2 ± 5.0 (3)[f]	0.41 ± 0.04*
2	1.15 ± 0.45 (4)[g]	20.8 ± 8.1**	48.3 ± 7.5 (3)[h]	0.25 ± 0.04*
3	5.04 ± 2.31 (3)[d]	4.76 ± 2.18**	113 ± 53 (3)[d]	0.21 ± 0.09*
4	0.49 ± 0.12 (3)[i]	24.5 ± 6.0***	75.1 ± 6.2 (3)[j]	0.43 ± 0.04*

[a]The values of K_d and relative binding affinities (relative receptor-binding affinity is defined as (K_d of human insulin or IGF-1/K_d of analog) × 100) of human IGF-1, insulin, and the analogs were determined for human IGF-1R in membranes of mouse fibroblasts and human IR-A in membranes of human IM-9 lymphocytes. Asterisks indicate that binding of the ligand differs significantly from that of IGF-1 (*$p < 0.05$; **$p < 0.01$; ***$p < 0.001$). [b]From Vikova et al. (ref 57). [c]From Krizkova et al. (ref 55). [d]Relative to human insulin K_d value of 0.24 ± 0.05 (n = 5). [e]Relative to human IGF-1 K_d value of 0.24 ± 0.10 (n = 5). [f]Relative to human insulin K_d value of 0.20 ± 0.04 (n = 5). [g]Relative to human IGF-1 K_d value of 0.24 ± 0.12 (n = 5). [h]Relative to human insulin K_d value of 0.12 ± 0.04 (n = 3). [i]Relative to human IGF-1 K_d value of 0.12 ± 0.01 (n = 5). [j]Relative to human insulin K_d value of 0.32 ± 0.09 (n = 4).

the cycloadditions at equimolar ratio of the precursor chains gave lower yields than the reactions with 2-fold molar excess of the azido chains. However, the optimum ratio of azido and propargyl precursors for **3b** was 1:1. Moreover, the use of more than 0.5 μmol (about 2 mg) of the yield-limiting propargyl-containing chain was ineffective. As a result, several click reactions for each analog were preformed to accumulate a sufficient amount of the material for their functional testing. The yields of optimized click reactions were typically about 16%, 18%, and 7% for **2c**, **3b**, and **4c**, respectively, after HPLC purification.

The final part of the synthetic work was focused on the optimization of an efficient, and proper/native, formation of the disulfide bonds in single-chain precursors **2c**, **3b**, and **4c**. Initially, an access of iodine in an acetic/hydrochloric acid mixture was used to cleave the Acm groups from Cys side chains in **2c** (Figure S2).[30] However, this was ineffective, as the majority of the Acm groups remained uncleaved, even after 4 h. Therefore, silver triflate was employed for the removal of the Acm groups, without the purification of an intermediate product. Subsequently, the free −SH groups were "liberated" from the Ag^+ salt by the gaseous H_2S, and the precipitated Ag_2S was removed by centrifugation. We followed here our successful application of such an approach for the removal of copper from synthesized compounds after click reactions.[58−60] Finally, the dilution of the supernatant, and the removal of an excess of the reductive H_2S gas, was followed by a slow air oxidation of the peptide, and its biomimetic folding, and the products **2**, **3**, and **4** were isolated by RP-HPLC. The typical yields of this last synthetic step were about 8% (0.5 mg) for **2**, 5.7% (0.27 mg) for **3**, and 1.7% (0.12 mg) for **4** (Figures S2−S4), which provided sufficient material for their biological characterization.

In summary, during the synthesis of peptide chain precursors and analogs, we encountered problems with the aspartimide formation in peptide **2a** and partly also with the oxidation of Met59 in peptide **2b**. We also found that *S*-sulfonate protection is not compatible with Cu^I-catalyzed click reaction and that simultaneous cleavage of six Acm-protecting groups in molecules of precursors with an access of I_2 was ineffective and had to be rectified by the use of silver triflate, followed by the removal of Ag^+ with a gaseous H_2S.

Functional Characterization of the analogs. *Binding Affinities to the Receptors.* The analogs **2**−**4**, and human insulin and IGF-1 as controls, were tested for their binding to human IGF-1R in membranes of mouse fibroblasts and to human IR-A in membranes of human IM-9 lymphocytes (Table 1, with the representative binding curves in Figures S5 and S6, respectively).

The two-chain analog **1** has significantly impaired binding for IGF-1R of only about 3.5% of the native IGF-1. Similar low binding (4.8%) was also detected for a single-chain analog **3**, in which Arg36 and Arg37 were replaced with β-azido-alanine and propargylglycine, respectively, connected by a triazole link, and with Met59Nle mutation. Interestingly, analog **2**, a "wild-type" homologue of **3** with preserved native Met59, showed markedly stronger 20.8% affinity than analog **3**.

The insertion of Arg36 and Arg39 in analog **4**, adjacent to the connecting triazole-containing 37−38 moiety, further enhanced IGF-1R binding affinity of this analog to almost 25% of the native IGF-1 binding.

Native human IGF-1 has only 1.0% binding affinity for IR-A compared to human insulin, but all analogs were even significantly weaker than human IGF-1 in binding to this receptor (Table 1).

Autophosphorylation of Receptors and Akt Activation. We also investigated the ability of analogs **1**−**4** to induce the autophosphorylation of IGF-1R (Figure 3A,C), and subsequent downstream phosphorylation of the Akt protein (pAkt) (Figure 3B,D), in response to their binding to this receptor. The potencies of the analogs were measured in IGF-1R-transfected 3T3 fibroblasts with high receptor population (Figure 3A,B) and, in parallel, in the non-transfected fibroblasts with a natural, that is, much lower, mouse IGF-1R population (Figure 3C,D). We also determined the ability of analogs **1**−**4** to stimulate the autophosphorylation of IR-A receptor in the IR-A-transfected fibroblasts (Figure 3E). The cells were stimulated for 10 min at 10^{-8} M concentration, and signals compared for all analogs (Figure 3A−E). Subsequently, the dose−response curves were measured for each analog (Figure 3F).

DOI: 10.1021/acs.jmedchem.7b01331
J. Med. Chem. 2017, 60, 10105−10117

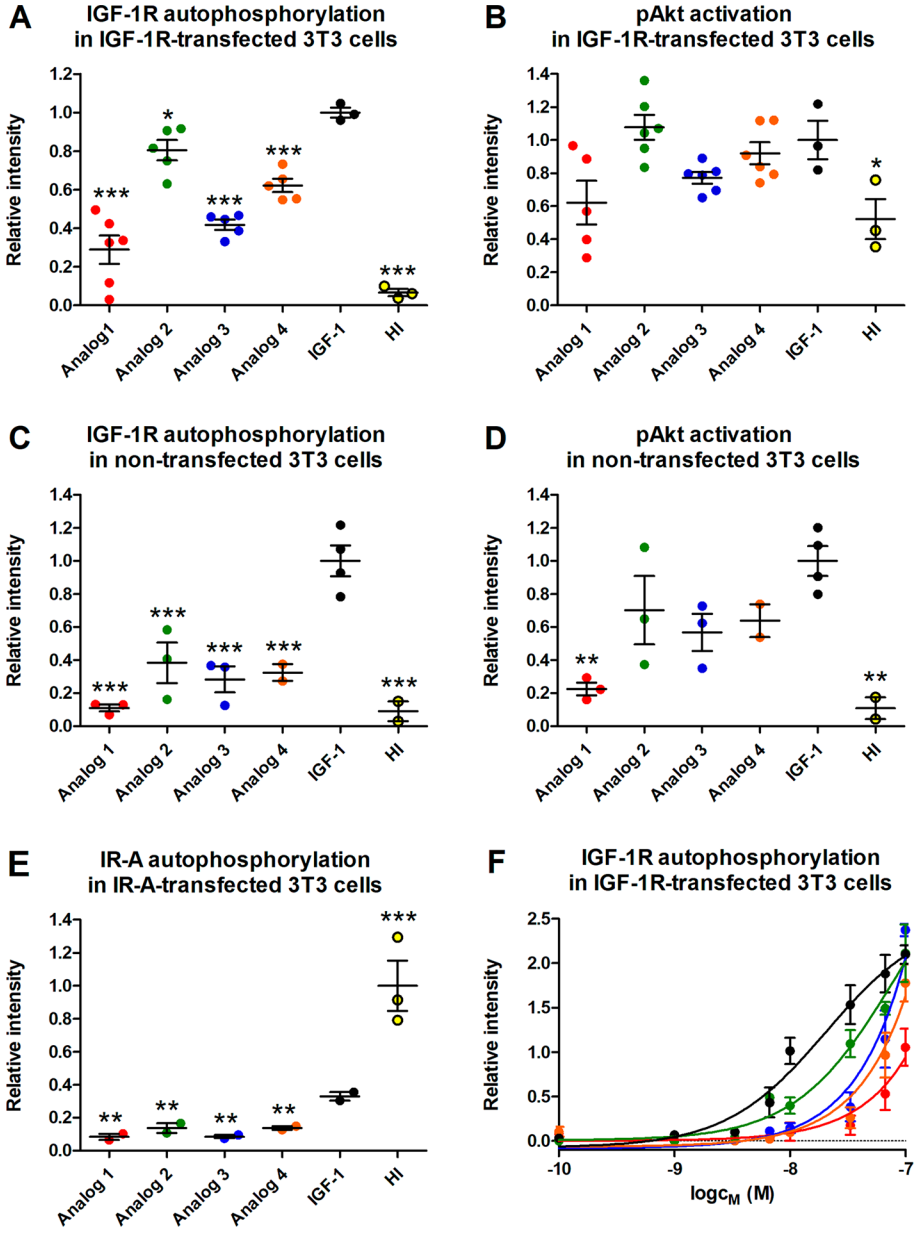

Figure 3. Receptor autophosphorylation and pAkt activation induced by analogs **1**–**4**, human IGF-1, and human insulin (HI). In (A–E), the cells were stimulated for 10 min with proteins at 10^{-8} M concentration only. In (F), the dose responses for proteins at several different concentrations were determined. In all panels, the same color scheme was used: human IGF-1 in black, analog **1** in red, analog **2** in green, analog **3** in blue, analog **4** in orange, and human insulin (HI) in yellow. (A) IGF-1R autophosphorylation in IGF-1R-transfected 3T3 fibroblasts. (B) pAkt activation in IGF-1R-transfected 3T3 fibroblasts. (C) IGF-1R autophosphorylation in non-transfected 3T3 fibroblasts. (D) pAkt activation in non-transfected 3T3 fibroblasts. (E) IR-A autophosphorylation in IR-A-transfected 3T3 fibroblasts. In most cases, the scatter plots show means ± SD of several independent measurements. However, in some cases where a low amount of material was available (for analog **4** in C–D), the plots show mean ± range calculated from two measurements. HI is human insulin. (F) Concentration-dependent effects of analogs on IGF-1R autophosphorylation in IGF-1R-transfected 3T3 fibroblasts. Asterisks indicate that phosphorylation of the receptor or Akt induced by the ligand differs significantly from that of IGF-1 (*$p < 0.05$; **$p < 0.01$; ***$p < 0.001$).

In general, the abilities of the analogs to stimulate autophosphorylation of IGF-1R and phosphorylation of intracellular Akt protein paralleled their IGF1-R binding affinities. The lowest IGF-1R autophosphorylation was observed for the two-chain analog **1** (4% binding) and for analog **3** with Met59Nle substitution (5% binding). However, interestingly, the analog **2** that lacks Arg36 and Arg37 activates IGF-1R somehow more strongly than analog **4**, which has Arg36 and Arg39 (Figure 3A), despite their reversed binding affinities of 21% and 24%, respectively. The ability of these analogs to activate/phosphorylate Akt protein follows this trend, although the differences between **2** and **4** are less significant here and similar to the native IGF-1 (Figure 3B). We compared the data measured for analogs **2** and **4**, using the two-tailed *t* test to determine the statistical significance of the observed differences, and only the stimulation of autophosphorylation of IGF-1R in transfected fibroblasts appeared statistically significant ($p = 0.02$), while the difference in binding activities was negligible ($p = 0.82$). In general, it appears that the transfected cells (Figure 3A,B) respond more

DOI: 10.1021/acs.jmedchem.7b01331
J. Med. Chem. 2017, 60, 10105–10117

sensitively to the stimulation with analogs than the non-transfected cells (Figure 3C,D), and this trend is visible especially in Akt activation (Figure 3B,D). It seems that higher sensitivity of the transfected cells alleviates the differences in binding affinities of analogs.

All analogs are also less potent than native IGF-1 in the stimulation of IR-A autophosphorylation in IR-A-transfected cells (Figure 3E).

Finally, the dose−response curves of IGF-1R autophosphorylation ability of analogs **1**−**4** and IGF-1 (Figure 3F) indicate that all analogs are weaker than IGF-1, where analog **2** is the strongest and analog **1** is the weakest, without a major difference between **3** and **4**; all in general agreement with the previous results.

DISCUSSION

Chemistry. The low yield (0.6%) of the recombination reaction, that is, a biomimetic formation of disulfides, for analog **1** is similar to the rather poor yields of some insulin analogs prepared previously and is significantly lower than typical yields for native human insulin (∼10%).[43] The poor folding ability of two separate chains of IGF-1 is also reflected in the complexity of the byproducts in the reaction mixture, where we identified, for example, a misfolded, inactive, but correct molecular mass, analog; the active analog **1** was found there as a rather minor peak (Figure S9). Misfolded and inactive IGF-1 molecules, specifically with "swapped" pairs of disulfides, that is, Cys6-Cys47 and Cys48-Cys52, instead of the correct Cys6-Cys48 and Cys47-Cys52, were identified previously in preparations of synthetic IGF-1 and its analogs.[20] However, the particularly poor yield of **1** clearly indicates the importance of a single-chain form of IGF-1 for its effective folding. Nevertheless, the amounts of analog **1** were sufficient for its biological characterization, especially with the recycling of chains **1a** and **1b** and repetition of the reaction.

We assumed that the single-chain IGF-1 analogs, with six free -SH groups, will oxidize themselves to a native conformation and that better folding properties of the single, rather than two-chain, IGF-1 analogs can be expected. However, as mentioned above, the 70-amino acid chain of IGF-1 is too long for an efficient solid-phase peptide synthesis. Therefore, we investigated here the possibility of connecting two IGF-1 fragments by Cu^{I}-catalyzed 1,3-dipolar cycloaddition of azides and alkynes, which would generate 1,2,3-triazole in the main-chain of IGF-1 analog. A similar approach was used by Valverde et al.[27] to connect three fragments of cysteine-protease protein inhibitor cystatin (98 amino acids). However, this did not require the formation of native disulfide bonds in this protein. As 1,4-disubstituted 1,2,3-triazoles are considered to be good mimics of the peptide bond,[28] it might be possible that their incorporation into the peptide chain in the IGF-1 C domain could be tolerated by IGF-1R. We were also encouraged here by our similar approach in the cross-linking of insulin B-chain with 1,2,3-triazole bridges, in which some highly potent IR analogs were obtained.[57]

Our first attempts at the clicking of two IGF-1 fragments involved the use of IGF-1 fragment 1−36 with β-azido alanine at position 36 and the IGF-1 fragment 37−70 with the propargyl glycine at position 37; all cysteines in these peptides were protected as *S*-sulfonates, which assured their good solubility and better separation on the HPLC. However, all our experiments (not shown) for connecting these fragments by Cu^{I}-catalyzed click reaction were unsuccessful (Figure S1). We concluded that the *S*-sulfonate groups are incompatible with the reaction, probably due to the *S*-sulfonate-copper chelation, which could lead to an undesired Cu-mediated folding of IGF-1 chains and steric blocking of the azido and alkyne groups, making them inaccessible for cycloaddition.

For this reason, we changed the Cys-protection strategy, synthesizing peptide chains with acetamidomethyl-protected cysteines, assuming that the Acm protection should not interfere with the clicking step, offering also several different alternative deprotections.[61] Unfortunately, the first synthesis of **2a** was hampered by a considerable amount of other, hardly separable, byproducts, identified as racemized aspartimides at positions Asp20-Arg21 (i.e., peptide **2ax**, see Figures S2, S12, and S28). The appearance of Asp-Arg aspartimides is rather rare, but not unusual in peptide chemistry,[62] as the Arg(Pbf)/Cys(Acm) protection strategy may promote this side reaction to a greater extent.[63] To test such a scenario in our chemical environment, we performed a model experiment (Supporting Information, pp 27−28) in which, with a model peptide **7**, Phe-Val-Cys(Acm)-Gly-Asp(O*t*Bu)-Arg(Pbf), we were able to generate and characterize (Figures S29, S30 and Scheme S1, Tables S1−S3) racemized aspartimides that were similar to the ones found in **2ax**. Therefore, we used a Fmoc-Asp(OEpe) derivative,[64] which helped to eliminate this problem in **2a** and **4a**. Hence, it seems that the formation of Asp20-Arg21 aspartimide in **2ax** was both sequence and side-chain protection-type dependent, as such byproducts were not observed in **1a**, **2b**, **3a**, and **4b**.

As mentioned above, the effective reactions and isolation of the products in the cycloaddition step required a reaction setup with a high excess of $CuSO_4$/ascorbate in water-*t*BuO,[56,57] but the addition of some click accelerators[65,66] or reactions in organic solvents[25] did not lead to the desired products. It is possible that the participation of bulky copper chelating agents like TBTA or THPTA is not favorable for steric reasons, if large peptide precursors are used. The failure of CuBr or CuI/DIPEA strategy in DMF could be due to a need for an effective protein hydration that is better in water-*t*BuOH. Although all reactions performed here were ineffective if they were scaled up above ∼2−4 mg per chain, some amount of the precursors could be recycled, and the reactions repeated. Both single-chain peptides without arginines in the proximity of the azido and alkyne precursor residues (**2c** and **3b**) gave better yields than peptide **4c** with the triazole-neighboring arginines. This could be due some steric shielding of the azido and alkyne moieties by the bulky arginine side chains.

Overall, we were able to prepare full-length IGF-1 chains on a preparative scale, still within reasonable yield ranges (7−18%). Our results underline the difficulty of click reactions where both precursors are large peptides, or proteins, compared to click reactions with small peptides/molecules, which usually proceed quickly and quantitatively.[25,26]

The final synthetic steps, that is, the deprotection of cysteines and the formation of physiological S−S bridges, were crucial for the success of the synthesis. Interestingly, the use of iodine in acetic acid/HCl[61] was not successful here, due to an incomplete cleavage of the Acm groups. One of the reasons for this could be the presence of six Acm groups accumulated in each molecule of the precursor, while only two Acm groups are usually simultaneously deprotected by I_2 for a directed formation of the disulfide.[30] For this reason, we used silver triflate, instead of I_2, for the cleavage of the Acm groups, without the purification of an intermediate product. Interest-

DOI: 10.1021/acs.jmedchem.7b01331
J. Med. Chem. 2017, 60, 10105−10117

ingly, this three-step procedure was relatively effective and successful, providing 6−8% yields for analogs **2** and **3**, which are comparable to our yields of syntheses of human insulin from its separate A and B chains (∼10%). However, calculated for a single folding step,[43] they were also much better than the ∼0.6% yields for the two-chain IGF-1 analog **1**. The less effective (1.7%) folding of analog **4** may result from the presence of Arg36 and Arg39 in this analog and, consequently, from a longer C domain than in **2** and **3**. It seems that the insertion of two additional Arg residues, rather than the presence of the triazole-containing connecting moiety, lowered the folding efficiency of this IGF-1 precursor. The folding of **2**−**4** was accompanied by the appearance of inactive misfolded "swapped" products (Figure S16), but to a lesser extent than in the case of **1** (Figure S9), certainly due to the single-chain character of precursors for **2**−**4**.

The clicked polypeptides reported here are, to our knowledge, unique examples of the use of triazole-forming chemistry for the preparative production of large peptides/small proteins (relative molecular weights about 8000 Da), with a native pattern of disulfide bridges. The middle position of the connecting triazole bridge in the protein main chain further validates the results. Moreover, the only few examples of true proteins with main-chain triazoles that were reported[27,67] did not contain disulfide bridges, which present additional challenges to such an approach.

Biology. Analog **1** retained some IGF-1R binding affinity, but its binding potency was severely impaired (3.5%) in comparison with the potency of the native IGF-1 (Table 1). This strongly suggests that the cleavage of Arg36-Arg37 peptide bond, if it occurs in vivo, is not a part of IGF-1 processing, but is rather a degradation-like step of this hormone, which leads to a much less active protein. Whether such cleavage represents some physiological attenuation of IGF-1 activity cannot be excluded, but it requires further, complex studies on this hormone, especially on in vivo-derived material.

The incorporation of the triazole bridge formed from β-azido-alanine at 36 and propargylglycine at 37 reduced the binding affinity of the analog **2** to about 21% of the binding affinity of the native IGF-1. However, this affinity drop is less significant than the effect of Ala36-Ala37 mutation of this hormone, which reduced its receptor binding to about 5%.[47] Therefore, it seems that the loss of Arg36-Arg37 in **2** is, somehow, compensated for by the triazole ring and/or the neighboring ethyl carboxymido (at 36) and ethyl amino (at 37) moieties. Some insight into the functional differences of the analogs **1**−**4** may be facilitated by a direct comparison of their connecting motifs shown in Figure 4. In **2**, this motif is three atoms longer than the peptide bond of the native IGF-1, and the only difference between analog **2** and **3** is Met59Nle mutation in analog **3**. This exchange reduced the IGF-1R affinity of the analog **3** to 5%, in agreement with the work of Shooter et al.,[68] where Met59Phe mutation resulted in the 17-fold decrease in IGF-1R binding. Therefore, analog **3** further highlights the importance of the sulfur atom in Met59 for receptor binding, which is not compensated for in **3** by the Nle alkyl chain. The highest IGF-1R binding affinity in the series from Table 1 was found for analog **4** (almost 25% of native IGF-1). However, statistical analysis (see above) showed that the difference in binding affinities of **4** and **2** is not significant, hence, both analogs are rather similar in this aspect. Although analog **4** retains arginines in the C-loop, they are at sites 36 and 39, not at their native positions 36−37 (Figures 2 and 4).

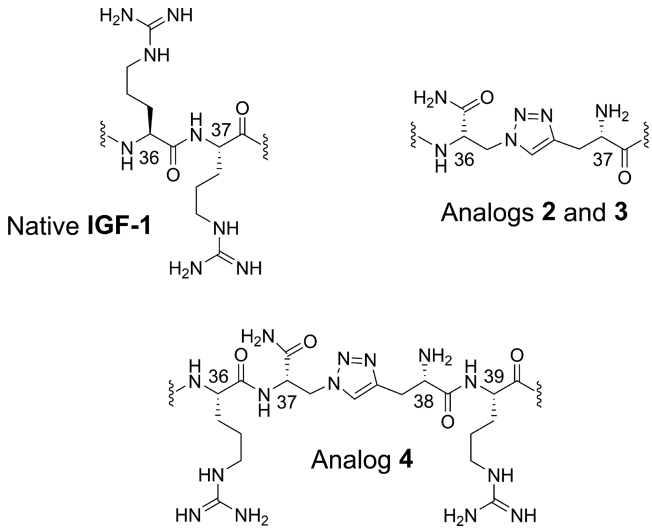

Figure 4. Comparison of the connecting motifs at positions 36−37 or 37−38 in analogs **2**−**4** with the native human IGF-1. Cα atoms are marked by residue numbers.

Therefore, the Cα atoms of the arginines in **4** are separated by eight extra backbone atoms plus triazole ring and carboxamide and amino moiety. Interestingly, this extension did not reduce the binding affinity of this analog in comparison with analog **2**, indicating a relative tolerance of IGF-1R for the modifications in this part of the C domain. However, it is also possible that at least one of the Arg36/Arg39 in **4** (e.g., Arg36) occupies a similar position on the receptor as one of the natives Arg36−37. This result opens up new possibilities for the use of different side chains, and motifs, at positions adjacent to the triazole ring, that is, 36 and 37 in **2** and 37 and 38 in **4**. However, such approaches depend on the development of available functionalized azides and alkynes suitable for the solid-phase peptide synthesis.

All analogs **1**−**4** have reduced binding affinities for the isoform A of the insulin receptor (Table 1) compared to native IGF-1. However, it seems that this decrease (21−43% of native IGF-1) is lower than for the IGF-1R (3−25% of native IGF-1), indicating that the C domain of IGF-1 is less important for IR-A binding than for an effective hormone complex formation with the IGF-1R.

The abilities of analogs **1**−**4** to induce the autophosphorylation of IGF-1R and IR-A and to activate the downstream Akt generally reflected their binding affinities for these receptors. This trend is especially visible in non-transfected fibroblasts, with a natural population of IGF-1R (Figure 3C,D). It seems that the high non-natural concentration of IGF-1R in IGF-1R-transfected fibroblasts is behind their higher sensitivity to the stimulation by the analogs, rather than differences in binding affinities of human IGF-1 for rat and human IGF-1R; this levels up the differences in binding affinities of analogs. The reason for this phenomenon could be in the "disproportional" populations/distributions of receptors and intracellular signaling proteins. In this respect, the native fibroblasts, with naturally lower population of IGF-1R, seem to be a better model. The only apparent exception here could be observed in a higher receptor stimulating activity of analog **2** than of analog **4** despite slightly reverse binding affinities. This "discrepancy" is interesting, but should be treated with caution, due to the low statistical significance of the differences between biological properties of analogs **2** and **4** mentioned above. Nevertheless,

DOI: 10.1021/acs.jmedchem.7b01331
J. Med. Chem. 2017, 60, 10105−10117

Scheme 1[a]

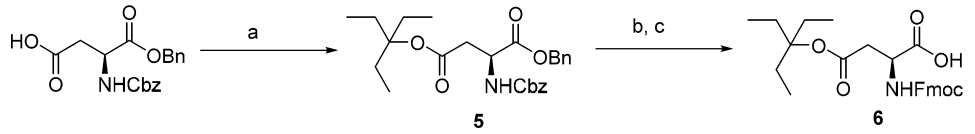

[a]Reagents, conditions, and yields (a) DIC, DMAP, 3-ethyl-3-pentanol, DCM 0 °C 1 h, then rt 48 h (91%); (b) 10% Pd/C, H_2, 10 psi, methanol 12 h; (c) Fmoc-OSu, $NaHCO_3$, water and dioxane, 0 °C 1 h, then rt overnight (65% over two steps).

we observed a similar phenomenon in the case of insulin-IGF hybrids, that is, human insulin molecules with the B chain prolonged for C domain amino acids of human IGF-2.[55] However, it is rather difficult to explain such a discrepancy without a structure of the analogs in a complex with the receptor, and even crystal/NMR structures of the analogs would provide only very limited clues. It is possible that only a complex with the so-called site 2 of IGF-1 receptor would shed light on the slightly differential activation/binding observed here, and only the structures of insulin and IGF-1 complexed with site 1 of the IR are currently available.[69,70] Nevertheless, as it was observed that differential binding kinetics of insulin-like analogs, that is, slower or faster k_{on} or k_{off} rates, can influence their metabolic or mitogenic biological responses,[71] this could be the case of the apparent differences between analogs **2** and **4**.

Finally, analogs **1**−**4** do not appear to possess the properties of IGF-1R antagonists or partial antagonists, as was observed for the IGF-1 Glu36-Glu37 mutant.[49,50] It is possible then that the antagonism observed for the Glu36-Glu37 IGF-1 analog results from a reversed, negatively charged glutamic acid's side chains, instead of the arginine basic guanidine groups, and that the replacement of the Arg36-Arg37 pair, by moieties shown in Figure 4, is not sufficient to elicit a similar antagonistic effect.

CONCLUSIONS

In summary, we developed a new method for the total chemical synthesis of human IGF-1 analogs, which entails a solid-phase synthesis of two IGF-1 precursor chains, and their ligation by Cu^I-catalyzed azide−alkyne cycloaddition chemistry. This relatively straightforward methodology presents a viable synthetic alternative to the previously established IGF synthetic strategies, which employed native ligation. The connection of two IGF-1 precursor chains by triazole-containing moieties was relatively well tolerated by IGF-1R and IR-A, both in terms of receptor binding and activation, and can thus represent a convenient and relatively straightforward synthetic strategy for the design of new analogs of this important human hormone with non-standard protein modifications. We also found that the disruption of the connectivity of the IGF-1 Arg36-Arg37 peptide bond deactivates this protein, hence it is unlikely that such cleavage represents a maturation step of this hormone in vivo.

EXPERIMENTAL SECTION

Unless otherwise stated, reagents and materials were obtained from commercial suppliers (Sigma-Aldrich-Fluka, Merck) and used without purification.

Solid-Phase Peptide Synthesis. Peptide chains were prepared by manual solid-phase synthesis in plastic syringes, equipped either with a Teflon frit or with ABI433A peptide synthesizer. Standard Fmoc amino acids (Iris Biotech, Gmbh, Germany) were used, and couplings were done with HBTU/DIPEA or DIC/HOBT reagents in DMF. Usually two couplings (60 min) with Fmoc-amino acids (3−5 equiv for manual synthesis and 10 equiv for automated synthesis) were done. In manual synthesis, the efficiency of the couplings was monitored by the Kaiser test, and the amount of cleaved Fmoc group (20% piperidine in DMF for 5 and 20 min) was determined spectrophotometrically (extinction coefficient 7040 M^{-1} cm^{-1} at 301 nm). Fmoc-Asp(OEpe)-OH was prepared as described in the Supporting Information and used for the syntheses of **2a** and **4a**. Fmoc-β-azido-(*S*)-Ala-OH was prepared as described by Pícha et al.[72]

The peptide chains with the C-terminal β-azido-(*S*)-Ala carboxamide, **2a** and **4a**, were synthesized on Rink amide AM LL resin or Nova PEG Rink amide (Merck-Novabiochem), respectively. Fmoc-(*S*)-propargylglycine-OH was purchased from Sigma-Aldrich-Fluka. The peptide chains **1a**, **1b**, **2b**, **3a**, and **4b** with a free carboxy terminus were synthesized on Wang-ChemMatrix LL resins, preloaded with Fmoc-Ala or Fmoc-Arg(Pbf) (PCAS BioMatrix Inc.). The peptides were cleaved with 91.5% TFA, 2.3% H_2O, 2.3% thioanisol, 2.3% phenol, 1.15% DODT, and 0.45% TIS for 2−4 h. Subsequently, the crude peptides were precipitated from the cold diethyl ether (in at least 10-fold excess), centrifuged, and dried. The precipitates of crude peptides **1a** and **1b** were immediately converted to *S*-sulfonates and subsequently desalted, as previously described in detail.[42,43] Finally, all peptide chains were purified by RP-HPLC.

Peptide and Compound Characterization. The precursor peptides (**1a**, **1b**, **2a**, **2b**, **2c**, **3a**, **3b**, **4a**, **4b**, and **4c**), and the resulting IGF-1 analogs **1**−**4** were purified and the purity of compounds analyzed by RP-HPLC. HRMS spectra of all compounds, peptides, and analogs were obtained on a FTMS mass spectrometer LTQ-orbitrap XL (Thermo Fisher, Bremen, Germany) in electrospray ionization mode. The purity of target compounds **1**−**4** was ≥95% (RP-HPLC, HR-MS). The identity and purity of analogs **1**−**4** were furthermore verified by N-terminal sequencing. Analytical data for all peptide precursors, IGF-1 analogs **1**−**4**, and conditions for NMR measurements of **2a** and model compounds **7** are provided in the Figures S7−S30, Tables S1−S3, and Scheme S1. Melting points of compounds **5** and **6** were determined on a Boetius block and are uncorrected. ^1H and ^{13}NMR spectra of compounds **5** and **6** were measured on a Bruker AVANCE-600 spectrometer (^1H at 600.13 MHz, ^{13}C at 150.9 MHz) in $CDCl_3$, DMSO-d_6, CD_3OD, or D_2O solution at 300 K. The 2D-H,H-COSY, 2D-H,C-HSQC and 2D-H,C-HMBC spectra were recorded and used for the structural assignment of proton and carbon signals. IR spectra of compounds **5** and **6** were recorded on Bruker IFS 55 Equinox apparatus.

Peptide ***1a***. The yield (RP-HPLC) was 4.3% (27 mg). HRMS-ESI: Monoisotopic M_r calcd for $C_{169}H_{253}N_{45}O_{60}S_4$ 4000.701, found 4000.677.

Peptide ***1b***. The yield (RP-HPLC) was 12.2% (51 mg). HRMS-ESI: Monoisotopic M_r calcd for $C_{162}H_{267}N_{49}O_{60}S_9$ 4146.683, found 4146.665.

Analog ***1***. Recombination of chains **1a** (17 mg, 4.27 μmol) and **1b** (33 mg, 7.95 μmol) was done according to the procedure previously described in detail.[42,43] The typical yield of the analog **1** (relative to chain **1a** as the limiting component of the reaction) after RP-HPLC purification was about 0.6% (0.2 mg). HRMS-ESI: Monoisotopic M_r calcd for $C_{331}H_{514}N_{94}O_{102}S_7$ 7661.597, found 7661.617.

Peptide ***2a***. When Fmoc-Asp(O*t*Bu)-OH was used, the yield (RP-HPLC) was 6.2% (22 mg). HRMS-ESI: M_r calcd for $C_{172}H_{256}N_{48}O_{55}S_2$ 3937.815, found 3937.818. The aspartimide derivative of **2a** (with an aspartimide bond at Asp20-Arg21, that is, peptide **2ax**, see in the Supporting Information) was purified (Figure

DOI: 10.1021/acs.jmedchem.7b01331
J. Med. Chem. 2017, 60, 10105−10117

S28) as well, and the yield was 8.6% (30 mg). HRMS-ESI M_r calcd for $C_{172}H_{254}N_{48}O_{54}S_2$ 3919.805, found 3919.809.

If Fmoc-Asp(OEpe)-OH (**6**) was used for the synthesis, the yield (RP-HPLC) was 10.1% (120 mg). HRMS-ESI: M_r calcd for $C_{172}H_{256}N_{48}O_{55}S_2$ 3937.815, found 3937.819. Undesired aspartimide byproduct was not found in this case.

Peptide ***2b***. The yield (RP-HPLC) was 18.5% (75 mg). HRMS-ESI M_r calcd for $C_{173}H_{280}N_{50}O_{52}S_5$ 4049.941, found 4049.945.

Peptide ***2c***. In general, the click reactions were performed according to the protocol previously published by Vikova et al.,[57] but with a few modifications. Briefly, the typical reaction mixture contained the linear peptide **2a** (4 mg, 1.02 μmol) and **2b** (2 mg, 0.49 μmol), which were dissolved in 4.5 mL of a *tert*-butanol:water mixture (2:1, v/v). Next, the ascorbic acid (5.5 μmol) and $CuSO_4 \cdot 5\ H_2O$ (4.80 μmol) were added in a minimum volume of water (the mixture was freshly prepared). The reaction mixture proceeded with stirring at 40 °C overnight. The precipitated product was removed from the reaction mixture by centrifugation and was purified using RP-HPLC (C4 column). The typical yield (RP-HPLC, relative to the chain **2b** as the limiting component of the reaction) was about 16% (0.6 mg). HRMS-ESI M_r calcd for $C_{345}H_{536}N_{98}O_{107}S_7$ 7987.756, found 7987.768.

Analog ***2***. Clicked peptide **2c** (6.6 mg, 0.83 μmol) was dissolved in 1 mL of TFA with 250 mM silver triflate and 25 mM anisole and allowed to react for 1 h in an ice bath. The deprotected peptide was removed from the solution by precipitation with cold diethyl ether. The crude peptide was dissolved (60 μM) in degassed 0.1 M Gly/NaOH buffer (pH 10.5), and then the reaction mixture was treated with gaseous H_2S[58−60] to remove Ag^+ ions from cysteine salts. The precipitated Ag_2S was removed by centrifugation. The supernatant, containing the peptide with free SH groups, was diluted to 30 μM concentration (by the same buffer) and purged with argon to remove the excess hydrogen sulfide. The reaction mixture was briefly purged with air and allowed to oxidize in an opened flask without stirring for 3 days at 4 °C. The crude target compound **2** was desalted on a C4-cartridge (Macherey-Nagel) and purified using RP-HPLC (C4 column). The yield (RP-HPLC) was 8% (0.5 mg). HRMS-ESI M_r calcd for $C_{327}H_{500}N_{92}O_{101}S_7$, 7555.486, found 7555.502.

Peptide ***3a***. The yield (RP-HPLC) was 15% (46 mg). HRMS-ESI M_r calcd for $C_{174}H_{282}N_{50}O_{52}S_4$ 4031.984, found 4031.988.

Peptide ***3b***. The compound was prepared from **3a** (2 mg, 0.5 μmol) and **2a** (2 mg, 0.51 μmol) according to the procedure described for **2c**. The typical yield (RP-HPLC) was about 18.5% (0.74 mg). HRMS-ESI M_r calcd for $C_{346}H_{538}N_{98}O_{107}S_6$ 7969.799, found 7969.801.

Analog ***3***. Analog **3** was prepared from **3b** (5 mg, 0.63 μmol) by the method described for **2**. The yield (RP-HPLC) was 5.7% (0.27 mg). HRMS-ESI M_r calcd for $C_{328}H_{502}N_{92}O_{101}S_6$ 7537.530, found 7537.551.

Peptide ***4a***. The yield (RP-HPLC) was 13.8% (170 mg). HRMS-ESI M_r calcd for $C_{178}H_{268}N_{52}O_{56}S_2$ for 4093.916, found 4093.923.

Peptide ***4b***. The yield (RP-HPLC) was 16.6% (140 mg; 33 μmol). HRMS-ESI M_r calcd for $C_{179}H_{292}N_{54}O_{53}S_5$ 4206.042, found 4206.047.

Peptide ***4c***. Peptide **4c** was prepared from peptides **4a** (4 mg, 0.98 μmol) and **4b** (2 mg, 0.48 μmol) by the method described for **2c**. The typical yield (RP-HPLC, relative to the chain **4b** as the limiting component of the reaction) was 7.3% (0.29 mg). MS-ESI M_r calcd for $C_{357}H_{560}N_{106}O_{109}S_7$ 8299.958, found 8299.987.

Analog ***4***. Analog **4** was prepared from **4c** (7.5 mg, 0.9 μmol) by the method described for analog **2**. The yield (RP-HPLC) was 1.7% (0.12 mg). HRMS-ESI M_r calcd for $C_{339}H_{524}N_{100}O_{103}S_7$ 7867.688, found 7867.709.

(2S)-N-Benzyloxycarbonylaspartic Acid 1-Benzyl-4-((3-ethyl)-pent-3-yl)ester ***5***. Intermediate **5** was prepared using a slightly modified method described previously in a patent.[64] Briefly, DIC (870 μL; 5.63 mmol) was added under stirring and ice-cooling to a solution of Cbz-Asp-OBn (5 g; 14 mmol) and DMAP (0.34 g; 2.8 mmol), and 3-ethyl-3-pentanol (4.8 g; 42 mmol) in 25 mL DCM was added DIC. The cooling was finished, and the mixture was allowed to react at rt 16 h. Addition of DIC (870 μL) was repeated twice, and the total reaction time was 48 h. The excess of DIC was eliminated by quenching with glacial acetic acid, and the volatile material was evaporated in vacuo to give a yellow residue, which was purified by flash chromatography on silica gel using a linear gradient of ethyl acetate in petroleum ether. Yield 5.8 g (91%). Colorless oil. R_f = 0.74 (20% ethyl acetate/toluen). $[\alpha]_D^{20}$ = +14° (*c* = 0.669 ; $CHCl_3$). ^{1}H NMR (500 MHz, $CDCl_3$): 0.70 (9H, t, *J* = 7.5, 3× CH_3), 1.71 (6H, q, *J* = 7.5, 3× CH_2), 2.96 (1H, dd, *J* = 17.2 and 4.5, CO-CHaHb-), 2.77 (1H, dd, *J* = 17.2 and 4.5, CO-CHaHb-), 4.56 (1H, dt, *J* = 8.8, 4.5 and 4.5, > CH-N), 5.05 (1H, d, *J* = 12.2, O-CHaHb-), 5.08 (1H, d, *J* = 12.2, O-CHaHb-), 5.10 (1H, d, *J* = 12.4, O-CHaHb-), 5.14 (1H, d, *J* = 12.4, O-CHaHb-), 5.77 (1H, d, *J* = 8.7, -NH-CO), 7.25−7.30 (10H, m, 2× C_6H_5); ^{13}C NMR (125.7 MHz, $CDCl_3$): 7.53 (3× CH_3); 26.63 (3× CH_2); 37.27 (CH_2); 50.53 (CH-N); 66.95 and 67.40 (2× CH_2-O), 90.06 (C-O), 127.95(2), 128.08, 128.17(2), 128.32, 128.45(2) and 128.49(2) (10× Ar ═CH-), 135.18 and 136.18 (2× Ar > C═), 155.98 (N-CO), 169.61 and 170.75 (2× O-CO). IR (CCl_4) ν_{max} cm^{-1} 3433 m, 3353 m (NH); 2972 s, 2883 m, 1380 s (CH_3); 2943 s (CH_2); 1751 vs + br (C═O) esters; 1727 vs (C═O) carbamate; 3091 w, 3066 w, 3034 w, 1500 s, 1456 s, 1175 s, 1028 s, 1003 s, 737 s, 697 m (ring). HRMS (ESI) calcd for $C_{26}H_{33}O_6NNa$ $[M + Na]^+$ 478.220, found: 478.220.

The synthesis of Fmoc-Asp(OEpe)-OH **6** is summarized in Scheme 1.

(2S)-N-((9H-Fluoren-9-ylmethoxy)carbonyl))aspartic acid 4-((3-ethyl)pent-3-yl)ester ***6***. Intermediate **5** (6.9 g; 15.1 mmol) was charged to a nitrogen flushed glass pressure bottle, dissolved in 80 mL of methanol, and then 500 mg of 10% Pd/C was added. The mixture was vigorously stirred and allowed to react under the atmosphere of hydrogen (15 psi) at RT for 12 h. TLC analysis (50% ethyl acetate/toluen) revealed that the starting compound had completely disappeared. The catalyst was filtered off through Celite, and the filter cake was washed with 100 mL of methanol. The filtrate was evaporated in vacuo to give 3.5 g of light brown residue, which was immediately dissolved in 50 mL of aqueous solution of $NaHCO_3$ (2.5 g; 30.2 mmol). The flask was placed in an ice bath, and Fmoc-OSu (5.1 g; 15.1 mmol) in 50 mL of dioxane was added dropwise under stirring. After the addition of the total amount of Fmoc-OSu, stirring continued for 1 h at 0 °C and then overnight at room temperature. Thereafter, 10% aqueous solution of citric acid was added to the reaction mixture until pH ∼3−4 was reached, followed by 200 mL water. The solution was transferred to a separator funnel and extracted with 4 × 100 mL of ethyl acetate. Combined organic layers were washed consecutively with 2 × 50 mL water, 2 × 50 mL brine, and dried over anhydrous Na_2SO_4. The filtrate was evaporated to afford a dark yellow oil, which was purified by flash chromatography on silica gel, using a linear gradient of ethyl acetate in toluene. Yield 4.5 g (65% over two steps). Bright yellow semisolid. R_f = 0.67 (ethyl acetate-acetone-ethanol-water 6/1/1/0.5). $[\alpha]_D^{20}$ = −8.6° (*c* = 0.326 ; DMF). ^{1}H NMR (600 MHz, DMSO): 0.73 (9H, t, *J* = 7.5, 3× CH_3), 1.72 (6H, q, *J* = 7.5, 3× CH_2), 2.53 (1H, dd, *J* = 15.9 and 9.1, CO-CHaHb-), 2.78 (1H, dd, *J* = 15.9 and 4.6, CO-CHaHb-), 4.20 (t, *J* = 6.5, > CH-), 4.25 (3H, m, > CH-N and −CH_2-O), 7.38 (1H, br, -NH-CO), 7.31 (2H, m), 7.41 (2H, m), 7.69 (2H, m) and 7.88 (2H, m) (2× C_6H_4);^{13}C NMR (150.9 MHz, DMSO): 7.60 (3× CH_3); 26.50 (3× CH_2); 37.27 (CH_2); 46.83 (>CH-); 66.81 (CH_2 -O), 87.83 (C-O), 120.31(2), 125.44(2), 127.26(2) and 124.83(2) (8× Ar ═CH-), 140.91(2), 144.02 and 144.02 (4× Ar > C═), 155.98 (N-CO), 169.71 (O-CO). IR (CCl_4) ν_{max} cm^{-1} 3437 w, 3322 w (NH); 2971 m, 2887 m, 1380 m, 1370 m (CH_3); 2945 m, 2856 m (CH_2); 1727 vs+vbr (C═O) all carbonyles; 1505 s (amide II); 3068 w, 3042 w, 3021 w, 1600 m, 1478 m, 1452 m, 678 s (ring). HRMS (ESI) calcd for $C_{26}H_{31}O_6NNa$ $[M + Na]^+$ 476.204, found: 476.204.

Cell Cultures. Human IM-9 lymphocytes and NIH/3T3 mouse fibroblasts were obtained from ATCC. Mouse fibroblasts derived from IGF-1R knockout mice[73] and stably transfected with either human IGF-1 receptor (IGF-1R), or human insulin receptor isoform A (IR-A), were kindly provided by Professor A. Belfiore (University of Magna Grecia, Catanzaro, Italy) and Professor R. Baserga (Thomas Jefferson University, Philadelphia, Pennsylvania, USA). IM-9 cells were grown in RPMI 1640 media with 10% fetal bovine serum. IGF-1R and IR-A cells were grown in DMEM media with 5 mM glucose with 10% fetal bovine serum and 0.3 μg/mL puromycin. NIH/3T3 cells were grown in DMEM media with 10% bovine serum albumin. All media

DOI: 10.1021/acs.jmedchem.7b01331
J. Med. Chem. 2017, 60, 10105−10117

were further supplemented with 2 mM L-glutamine, 100 U/mL penicillin and 100 μg/mL streptomycin, and the cells were grown in humidified air with 5% CO_2 at 37 °C.

Receptor-Binding Studies. *Human IM-9 Lymphocytes (Human IR-A Isoform).* Receptor-binding studies with the insulin receptor in membranes of human IM-9 lymphocytes (containing only human IR-A isoform) were performed and K_d values determined as described previously.[12,43] Binding data were analyzed using the Excel algorithms specifically developed for the IM-9 cells system in the laboratory of Prof. Pierre De Meyts (A. V. Groth and R. M. Shymko, Hagedorn Research Institute, Denmark, a kind gift from P. De Meyts), using the method of a non-linear regression, and a one-site fitting program, taking into account the potential depletion of the free ligand. Each binding curve was determined in duplicate, and the final dissociation constant (K_d) of an analog was calculated from at least three ($n \geq 3$) binding curves (K_d values), determined independently. The dissociation constant of human ^{125}I-insulin (PerkinElmer) was set to 0.3 nM.

Mouse Embryonic Fibroblasts (Human IGF-1R). Receptor binding studies with the human IGF-1 receptor in membranes of mouse embryonic fibroblasts derived from IGF-1R knockout mice and transfected with human IGF-1R were performed as described previously.[12,43] Binding data were analyzed, and the dissociation constant (K_d) was determined with GraphPad Prism 5 software, using a non-linear regression method and a one-site fitting program, taking into account potential depletion of free ligand. Each binding curve was determined in duplicate, and the final dissociation constant (K_d) of an analogue was calculated from at least three ($n \geq 3$) binding curves (K_d values) determined independently. The dissociation constant of human ^{125}I-IGF-1 (PerkinElmer) was set to 0.2 nM. Here we should note that the use of bovine serum albumin (e.g., Sigma-Aldrich A6003) void of "IGF-binding-like" proteins, which interfere with these binding assays, is essential for the preparation of the binding buffer.[74]

The significance of the changes in binding affinities of the analogs, related to the binding of IGF-1, was calculated using a two-tailed *t* test.

Receptor Phosphorylation Assay. *Cell Stimulation and Detection of Receptor phosphorylation.* Both were performed as previously described.[55] In brief, mouse fibroblasts (NIH/3T3, IR-A and IGF-1R) were seeded in 24-well plates (Schoeller) and incubated for 24 h. Cells were afterward starved for 4 h in serum-free media. The cells were stimulated with 10 nM concentrations of the ligands for 10 min. Proteins were routinely analyzed, using immunoblotting and horseradish peroxidase-labeled secondary antibodies (Sigma-Aldrich). The membranes were probed with antiphospho-IGF-1Rβ (Tyr1135/1136)/IRβ (Tyr1150/1151) and antiphospho-Akt (Thr308) (C31E5E) (Cell Signaling Technology). The blots were developed using the SuperSignal West Femto maximum sensitivity substrate (Pierce) and analyzed using the ChemiDoc MP Imaging System (Bio-Rad). Each experiment was repeated four times. The data were expressed as contribution of phosphorylation relatively to the human insulin (IR-A) respective IGF-1 (NIH/3T3 and IGF-1R) signal. The significance of the changes in stimulation of phosphorylation of receptors and related Akt-stimulation by the IGF-1 was calculated using one-way analysis of variance.

Ligand-Dose Response IGF-1R Autophosphorylation Levels. The levels were determined using In-Cell Western assay[75] adapted for chemiluminescence. The IGF-1R cells were plated at 20 000 cells/well in white 96-well Brand plates cell grade (Brand GMBH, Germany) and incubated for 24 h. Cells were afterward starved for 4 h in serum-free media and stimulated with dilutions of ligands (0−100 nM) for 10 min. After incubation, the medium was discarded, and the cells were fixed in 3.75% freshly prepared formaldehyde for 20 min. Cells were permeabilized with 0.1% Triton-X-100 in PBS for 5 min and blocked with 5% BSA in T-TBS for 1 h. Plates were incubated with antiphospho-IGF-1Rβ (Tyr1135/1136)/IRβ (Tyr1150/1151) overnight at 4 °C. Then plates were thoroughly washed with TBS, incubated with peroxidase-labeled antirabbit secondary antibody (Sigma) for 1 h at room temperature, and washed again. SuperSignal West Femto maximum sensitivity substrate was added to each well, and chemiluminescence was detected using the ChemiDoc MP Imaging System after 5 min. Data were subtracted from background values and expressed as contribution of phosphorylation relatively to the 10 nM IGF-1 signal. Control wells and wells stimulated with 10 nM IGF-1 were in tetraplicates on each plate. Experiments were repeated at least four times. Log(agonist) vs response curve fitting of data was carried out with GraphPad Prism 5 software.

■ ASSOCIATED CONTENT

Supporting Information

The Supporting Information is available free of charge on the ACS Publications website at DOI: 10.1021/acs.jmedchem.7b01331.

Figures S1−S4: Synthetic pathways for analogs **1**−**4**. Figures S5 and S6: binding curves of compounds with the receptors. Figures S7−S10, S12−S17, S19−S21, S23−S26: HPLC analyses of compounds. Figures S11, S18, S22 and S27: HRMS-ESI spectra of target compounds **1**−**4**. Characterization of the aspartimide derivatives of peptides **2a** and **7**: Figures S28−S30, Tables S1−S3, Scheme S1 (PDF)

■ AUTHOR INFORMATION

Corresponding Author

*Phone: +420 220183 441. E-mail: jiracek@uochb.cas.cz.

ORCID

Andrzej M. Brzozowski: 0000-0001-7426-8948

Jiří Jiráček: 0000-0003-3848-2773

Notes

The authors declare no competing financial interest.

■ ACKNOWLEDGMENTS

This work was supported by Medical Research Council Grant MR/K000179/1 (to A.M.B.). This work was also supported by the Research Project of the Czech Academy of Sciences RVO:61388963 (for the Institute of Organic Chemistry and Biochemistry).

■ ABBREVIATIONS USED

Acm, acetamidomethyl; c_M, molar concentration; DIC, *N*,*N*′-diisopropylcarbodiimide; DILP, *Drosophila* insulin-like peptide; DIPEA, *N*,*N*-diisopropylethylamine; DMF, dimethylformamide; DODT, 2,2′-(ethylenedioxy)diethanethiol; Epe, ethylpentyl; INSL, insulin-like peptide insulin receptor isoform A; IGF, insulin-like growth factor; IR-B, insulin receptor isoform B; IGF-1R, receptor for IGF-1; HBTU, *N*,*N*,*N*′,*N*′-tetramethyl-*O*-(1H-benzotriazol-1-yl)uronium hexafluorophosphate; HOBt, hydroxybenzotriazole; M_r, relative molecular weight; HRMS-ESI, high-resolution mass spectrometry electrospray ionization; RP-HPLC, reverse-phase high-performance liquid chromatography; TBTA, tris[(1-benzyl-1H-1,2,3-triazol-4-yl)methyl]-amine; TFA, trifluoroacetic acid; THPTA, tris(3-hydroxypropyltriazolylmethyl)amine; TIS, triisopropylsilane; Trt, trityl

■ REFERENCES

(1) Taniguchi, C. M.; Emanuelli, B.; Kahn, C. R. Critical nodes in signalling pathways: insights into insulin action. *Nat. Rev. Mol. Cell Biol.* **2006**, *7*, 85−96.

(2) Cohen, P. Timeline - the twentieth century struggle to decipher insulin signalling. *Nat. Rev. Mol. Cell Biol.* **2006**, *7*, 867−873.

(3) Denley, A.; Cosgrove, L. J.; Booker, G. W.; Wallace, J. C.; Forbes, B. E. Molecular interactions of the IGF system. *Cytokine Growth Factor Rev.* **2005**, *16*, 421−439.

DOI: 10.1021/acs.jmedchem.7b01331
J. Med. Chem. 2017, 60, 10105−10117

(4) Bluher, M.; Kahn, B. B.; Kahn, C. R. Extended longevity in mice lacking the insulin receptor in adipose tissue. *Science* **2003**, *299*, 572−574.
(5) Holzenberger, M.; Dupont, J.; Ducos, B.; Leneuve, P.; Geloen, A.; Even, P. C.; Cervera, P.; Le Bouc, Y. IGF-1 receptor regulates lifespan and resistance to oxidative stress in mice. *Nature* **2003**, *421*, 182−187.
(6) Gallagher, E. J.; LeRoith, D. Minireview: IGF, insulin, and cancer. *Endocrinology* **2011**, *152*, 2546−2551.
(7) Belfiore, A.; Frasca, F.; Pandini, G.; Sciacca, L.; Vigneri, R. Insulin receptor isoforms and insulin receptor/insulin-like growth factor receptor hybrids in physiology and disease. *Endocr. Rev.* **2009**, *30*, 586−623.
(8) Mayer, J. P.; Zhang, F.; DiMarchi, R. D. Insulin structure and function. *Biopolymers* **2007**, *88*, 687−713.
(9) Zaykov, A. N.; Mayer, J. P.; DiMarchi, R. D. Pursuit of a perfect insulin. *Nat. Rev. Drug Discovery* **2016**, *15*, 425−439.
(10) Vajo, Z.; Fawcett, J.; Duckworth, W. C. Recombinant DNA technology in the treatment of diabetes: insulin analogs. *Endocr. Rev.* **2001**, *22*, 706−717.
(11) Bright, G. M. Recombinant IGF-I: Past, present and future. *Growth Horm. IGF Res.* **2016**, *28*, 62−65.
(12) Hexnerova, R.; Krizkova, K.; Fabry, M.; Sieglova, I.; Kedrova, K.; Collinsova, M.; Ullrichova, P.; Srb, P.; Williams, C.; Crump, M. P.; Tosner, Z.; Jiracek, J.; Veverka, V.; Zakova, L. Probing receptor specificity by sampling the conformational space of the insulin-like growth factor II C-domain. *J. Biol. Chem.* **2016**, *291*, 21234−21245.
(13) Kent, S. B. H. Total chemical synthesis of proteins. *Chem. Soc. Rev.* **2009**, *38*, 338−351.
(14) Li, C. H.; Yamashiro, D.; Gospodarowicz, D.; Kaplan, S. L.; Vanvliet, G. Total synthesis of insulin-like growth factor-I (somatomedin-C). *Proc. Natl. Acad. Sci. U. S. A.* **1983**, *80*, 2216−2220.
(15) Iwai, M.; Kobayashi, M.; Tamura, K.; Ishii, Y.; Yamada, H.; Niwa, M. Direct identification of disulfide bond linkages in human insulin-like growth factor-I (IGF-I) by chemical synthesis. *J. Biochem.* **1989**, *106*, 949−951.
(16) Bagley, C. J.; Otteson, K. M.; May, B. L.; Mccurdy, S. N.; Pierce, L.; Ballard, F. J.; Wallace, J. C. Synthesis of insulin-like growth factor-I using N-methyl pyrrolidinone as the coupling solvent and trifluoromethane sulfonic-acid cleavage from the resin. *Int. J. Pept. Protein Res.* **1990**, *36*, 356−361.
(17) Luisier, S.; Avital-Shmilovici, M.; Weiss, M. A.; Kent, S. B. H. Total chemical synthesis of human proinsulin. *Chem. Commun.* **2009**, *46*, 8177−8179.
(18) Sohma, Y.; Hua, Q. X.; Whittaker, J.; Weiss, M. A.; Kent, S. B. H. Design and folding of [Glu(A4)(O(beta)Thr(B30))]insulin ("ester insulin"): a minimal proinsulin surrogate that can be chemically converted into human insulin. *Angew. Chem., Int. Ed.* **2010**, *49*, 5489−5493.
(19) Avital-Shmilovici, M.; Mandal, K.; Gates, Z. P.; Phillips, N. B.; Weiss, M. A.; Kent, S. B. H. Fully convergent chemical synthesis of ester insulin: determination of the high resolution X-ray structure by racemic protein crystallography. *J. Am. Chem. Soc.* **2013**, *135*, 3173−3185.
(20) Sohma, Y.; Pentelute, B. L.; Whittaker, J.; Hua, Q. X.; Whittaker, L. J.; Weiss, M. A.; Kent, S. B. H. Comparative properties of insulin-like growth factor 1 (IGF-1) and [Gly7D-Ala]IGF-1 prepared by total chemical synthesis. *Angew. Chem., Int. Ed.* **2008**, *47*, 1102−1106.
(21) Cottam, J. M.; Scanlon, D. B.; Karas, J. A.; Calabrese, A. N.; Pukala, T. L.; Forbes, B. E.; Wallace, J. C.; Abell, A. D. Chemical synthesis of a fluorescent IGF-II analogue. *Int. J. Pept. Res. Ther.* **2013**, *19*, 61−69.
(22) Tornoe, C. W.; Meldal, M. Peptidotriazoles: Copper(I)-Catalyzed 1,3-Dipolar Cycloadditions on Solid-Phase. In Proceedings of the *2nd International and the 17th American Peptide Symposium*; Lebl, M., Houghten, R. A., Eds.; 2001; pp 263−264.
(23) Rostovtsev, V. V.; Green, L. G.; Fokin, V. V.; Sharpless, K. B. A stepwise Huisgen cycloaddition process: Copper(I)-catalyzed regioselective "ligation" of azides and terminal alkynes. *Angew. Chem., Int. Ed.* **2002**, *41*, 2596−2599.
(24) Tornoe, C. W.; Christensen, C.; Meldal, M. Peptidotriazoles on solid phase: [1,2,3]-triazoles by regiospecific copper(I)-catalyzed 1,3-dipolar cycloadditions of terminal alkynes to azides. *J. Org. Chem.* **2002**, *67*, 3057−3064.
(25) Meldal, M.; Tornoe, C. W. Cu-catalyzed azide-alkyne cycloaddition. *Chem. Rev.* **2008**, *108*, 2952−3015.
(26) Pedersen, D. S.; Abell, A. 1,2,3-triazoles in peptidomimetic chemistry. *Eur. J. Org. Chem.* **2011**, *2011*, 2399−2411.
(27) Valverde, I. E.; Lecaille, F.; Lalmanach, G.; Aucagne, V.; Delmas, A. F. Synthesis of a biologically active triazole-containing analogue of cystatin a through successive peptidomimetic alkyne-azide ligations. *Angew. Chem., Int. Ed.* **2012**, *51*, 718−722.
(28) Valverde, I. E.; Bauman, A.; Kluba, C. A.; Vomstein, S.; Walter, M. A.; Mindt, T. L. 1,2,3-triazoles as amide bond mimics: triazole scan yields protease-resistant peptidomimetics for tumor targeting. *Angew. Chem., Int. Ed.* **2013**, *52*, 8957−8960.
(29) Wu, F. Z.; Mayer, J. P.; Gelfanov, V. M.; Liu, F.; DiMarchi, R. D. Synthesis of four-disulfide insulin analogs via sequential disulfide bond formation. *J. Org. Chem.* **2017**, *82*, 3506−3512.
(30) Karas, J. A.; Patil, N. A.; Tailhades, J.; Sani, M. A.; Scanlon, D. B.; Forbes, B. E.; Gardiner, J.; Separovic, F.; Wade, J. D.; Hossain, M. A. Total chemical synthesis of an intra-A-chain cystathionine human insulin analogue with enhanced thermal stability. *Angew. Chem., Int. Ed.* **2016**, *55*, 14743−14747.
(31) Liu, F.; Zaykov, A. N.; Levy, J. J.; DiMarchi, R. D.; Mayer, J. P. Chemical synthesis of peptides within the insulin superfamily. *J. Pept. Sci.* **2016**, *22*, 260−270.
(32) Hossain, M. A.; Rosengren, K. J.; Zhang, S. D.; Bathgate, R. A. D.; Tregear, G. W.; van Lierop, B. J.; Robinson, A. J.; Wade, J. D. Solid phase synthesis and structural analysis of novel A-chain dicarba analogs of human relaxin-3 (INSL7) that exhibit full biological activity. *Org. Biomol. Chem.* **2009**, *7*, 1547−1553.
(33) Zhang, S. D.; Hughes, R. A.; Bathgate, R. A. D.; Shabanpoor, F.; Hossain, M. A.; Lin, F.; van Lierop, B.; Robinson, A. J.; Wade, J. D. Role of the intra-A-chain disulfide bond of insulin-like peptide 3 in binding and activation of its receptor, RXFP2. *Peptides* **2010**, *31*, 1730−1736.
(34) Shabanpoor, F.; Hossain, M. A.; Ryan, P. J.; Belgi, A.; Layfield, S.; Kocan, M.; Zhang, S. D.; Samuel, C. S.; Gundlach, A. L.; Bathgate, R. A. D.; Separovic, F.; Wade, J. D. Minimization of human relaxin-3 leading to high-affinity analogues with increased selectivity for relaxin-family peptide 3 receptor (RXFP3) over RXFP1. *J. Med. Chem.* **2012**, *55*, 1671−1681.
(35) Hossain, M. A.; Haugaard-Kedstrom, L. M.; Rosengren, K. J.; Bathgate, R. A. D.; Wade, J. D. Chemically synthesized dicarba H2 relaxin analogues retain strong RXFP1 receptor activity but show an unexpected loss of in vitro serum stability. *Org. Biomol. Chem.* **2015**, *13*, 10895−10903.
(36) Lin, F.; Hossain, M. A.; Post, S.; Karashchuk, G.; Tatar, M.; De Meyts, P.; Wade, J. D. Total solid-phase synthesis of biologically active drosophila insulin-like peptide 2 (DILP2). *Aust. J. Chem.* **2017**, *70*, 208−212.
(37) Menting, J. G.; Gajewiak, J.; MacRaild, C. A.; Chou, D. H. C.; Disotuar, M. M.; Smith, N. A.; Miller, C.; Erchegyi, J.; Rivier, J. E.; Olivera, B. M.; Forbes, B. E.; Smith, B. J.; Norton, R. S.; Safavi-Hemami, H.; Lawrence, M. C. A minimized human insulin-receptor-binding motif revealed in a Conus geographus venom insulin. *Nat. Struct. Mol. Biol.* **2016**, *23*, 916−920.
(38) Du, Y. C.; Zhang, Y. S.; Lu, Z. X.; Tsou, C. L. Resynthesis of insulin from its glycyl and phenylalanyl chains. *Sci. Sin.* **1961**, *10*, 84−104.
(39) Ruegg, U. T.; Gattner, H. G. Reduction of S-sulfo groups by tributylphosphine - improved method for recombination of insulin chains. *Hoppe-Seyler's Z. Physiol. Chem.* **1975**, *356*, 1527−1533.
(40) Chance, R. E.; Hoffmann, J. A.; Kroeff, E. P.; Johnson, M. G.; Schirmer, E. W.; Bromer, W. W. The Production of Human Insulin Using Recombinant DNA Technology and a New Chain Combination Procedure. In Proceedings of the *7th American Peptide Symposium*;

DOI: 10.1021/acs.jmedchem.7b01331
J. Med. Chem. 2017, 60, 10105−10117

Rich, D. H., Gross, E., Eds.; Pierce Chemical Company: Rockford, IL, 1981; pp 721−728.
(41) Wang, S. H.; Hu, S. Q.; Burke, G. T.; Katsoyannis, P. G. Insulin analogs with modifications in the beta-turn of the B-chain. *J. Protein Chem.* **1991**, *10*, 313−324.
(42) Krizkova, K.; Veverka, V.; Maletinska, L.; Hexnerova, R.; Brzozowski, A. M.; Jiracek, J.; Zakova, L. Structural and functional study of the GlnB22-insulin mutant responsible for maturity-onset diabetes of the young. *PLoS One* **2014**, *9*, e112883.
(43) Kosinova, L.; Veverka, V.; Novotna, P.; Collinsova, M.; Urbanova, M.; Moody, N. R.; Turkenburg, J. P.; Jiracek, J.; Brzozowski, A. M.; Zakova, L. Insight into the structural and biological relevance of the T/R transition of the N-terminus of the B-chain in human insulin. *Biochemistry* **2014**, *53*, 3392−3402.
(44) Bayne, M. L.; Applebaum, J.; Underwood, D.; Chicchi, G. G.; Green, B. G.; Hayes, N. S.; Cascieri, M. A. The C region of human insulin-like growth factor (IGF) I is required for high affinity binding to the type 1 IGF receptor. *J. Biol. Chem.* **1989**, *264*, 11004−11008.
(45) Gill, R.; Wallach, B.; Verma, C.; Urso, B.; DeWolf, E.; Grotzinger, J.; MurrayRust, J.; Pitts, J.; Wollmer, A.; DeMeyts, P.; Wood, S. Engineering the C-region of human insulin-like growth factor-1: implications for receptor binding. *Protein Eng., Des. Sel.* **1996**, *9*, 1011−1019.
(46) Denley, A.; Bonython, E. R.; Booker, G. W.; Cosgrove, L. J.; Forbes, B. E.; Ward, C. W.; Wallace, J. C. Structural determinants for high-affinity binding of insulin-like growth factor II to insulin receptor (IR)-A, the exon 11 minus isoform of the IR. *Mol. Endocrinol.* **2004**, *18*, 2502−2512.
(47) Zhang, W.; Gustafson, T. A.; Rutter, W. J.; Johnson, J. D. Positively charged side chains in the insulin-like growth factor-1 C- and D-regions determine receptor binding specificity. *Oncol. Rep.* **1994**, *269*, 10609−10613.
(48) Jansson, M.; Andersson, G.; Uhlen, M.; Nilsson, B.; Kordel, J. The insulin-like growth factor (IGF)binding protein 1 binding epitope on IGF-I probed by heteronuclear NMB spectroscopy and mutational analysis. *J. Biol. Chem.* **1998**, *273*, 24701−24707.
(49) Saegusa, J.; Yamaji, S.; Ieguchi, K.; Wu, C. Y.; Lam, K. S.; Liu, F. T.; Takada, Y. K.; Takada, Y. The direct binding of insulin-like growth factor-1 (IGF-1) to integrin alpha v beta 3 is involved in IGF-1 signaling. *J. Biol. Chem.* **2009**, *284*, 24106−24114.
(50) Fujita, M.; Ieguchi, K.; Cedano-Prieto, D. M.; Fong, A.; Wilkerson, C.; Chen, J. Q.; Wu, M.; Lo, S. H.; Cheung, A. T. W.; Wilson, M. D.; Cardiff, R. D.; Borowsky, A. D.; Takada, Y. K.; Takada, Y. An integrin binding-defective mutant of insulin-like growth factor-1 (R36E/R37E IGF1) acts as a dominant-negative antagonist of the IGF1 receptor (IGF1R) and suppresses tumorigenesis but still binds to IGF1R. *J. Biol. Chem.* **2013**, *288*, 19593−19603.
(51) Brzozowski, A. M.; Dodson, E. J.; Dodson, G. G.; Murshudov, G. N.; Verma, C.; Turkenburg, J. P.; de Bree, F. M.; Dauter, Z. Structural origins of the functional divergence of human insulin-like growth factor-I and insulin. *Biochemistry* **2002**, *41*, 9389−9397.
(52) Vajdos, F. F.; Ultsch, M.; Schaffer, M. L.; Deshayes, K. D.; Liu, J.; Skelton, N. J.; de Vos, A. M. Crystal structure of human insulin-like growth factor-1: detergent binding inhibits binding protein interactions. *Biochemistry* **2001**, *40*, 11022−11029.
(53) Sitar, T.; Popowicz, G. M.; Siwanowicz, I.; Huber, R.; Holak, T. A. Structural basis for the inhibition of insulin-like growth factors by insulin-like growth factor-binding proteins. *Proc. Natl. Acad. Sci. U. S. A.* **2006**, *103*, 13028−13033.
(54) Jiracek, J.; Zakova, L. Structural perspectives of insulin receptor isoform-selective insulin analogs. *Front. Endocrinol.* **2017**, *8*, 167.
(55) Krizkova, K.; Chrudinova, M.; Povalova, A.; Selicharova, I.; Collinsova, M.; Vanek, V.; Brzozowski, A. M.; Jiracek, J.; Zakova, L. Insulin-insulin-like growth factors hybrids as molecular probes of hormone:receptor binding specificity. *Biochemistry* **2016**, *55*, 2903−2913.
(56) Isaad, A. L.; Papini, A. M.; Chorev, M.; Rovero, P. Side chain-to-side chain cyclization by click reaction. *J. Pept. Sci.* **2009**, *15*, 451−454.
(57) Vikova, J.; Collinsova, M.; Kletvikova, E.; Budesinsky, M.; Kaplan, V.; Zakova, L.; Veverka, V.; Hexnerova, R.; Avino, R. J. T.; Strakova, J.; Selicharova, I.; Vanek, V.; Wright, D. W.; Watson, C. J.; Turkenburg, J. P.; Brzozowski, A. M.; Jiracek, J. Rational steering of insulin binding specificity by intra-chain chemical crosslinking. *Sci. Rep.* **2016**, *6*, 19431.
(58) Vanek, V.; Picha, J.; Fabre, B.; Budesinsky, M.; Lepsik, M.; Jiracek, J. The development of a versatile trifunctional scaffold for biological applications. *Eur. J. Org. Chem.* **2015**, *2015*, 3689−3701.
(59) Fabre, B.; Picha, J.; Vanek, V.; Budesinsky, M.; Jiracek, J. A CuAAC-hydrazone-CuAAC trifunctional scaffold for the solid-phase synthesis of trimodal compounds: Possibilities and limitations. *Molecules* **2015**, *20*, 19310−19329.
(60) Fabre, B.; Picha, J.; Vanek, V.; Selicharova, I.; Chrudinova, M.; Collinsova, M.; Zakova, L.; Budeginsky, M.; Jiracek, J. Synthesis and evaluation of a library of trifunctional scaffold-derived compounds as modulators of the insulin receptor. *ACS Comb. Sci.* **2016**, *18*, 710−722.
(61) Isidro-Llobet, A.; Alvarez, M.; Albericio, F. Amino acid-protecting groups. *Chem. Rev.* **2009**, *109*, 2455−2504.
(62) Behrendt, R.; White, P.; Offer, J. Advances in Fmoc solid-phase peptide synthesis. *J. Pept. Sci.* **2016**, *22*, 4−27.
(63) Subiros-Funosas, R.; El-Faham, A.; Albericio, F. Aspartimide formation in peptide chemistry: occurrence, prevention strategies and the role of N-hydroxylamines. *Tetrahedron* **2011**, *67*, 8595−8606.
(64) Behrendt, R.; Willibald, J.; White, P. New Aspartic Acid Derivatives Useful for Synthesizing Peptide Which is Useful for Treatment of Crohn's Disease and Osteoporosis and as Adjuvant Therapy in Chemotherapy. European patent EP2886531, 2015.
(65) Hong, V.; Presolski, S. I.; Ma, C.; Finn, M. G. Analysis and optimization of copper-catalyzed azide-alkyne cycloaddition for bioconjugation. *Angew. Chem., Int. Ed.* **2009**, *48*, 9879−9883.
(66) Chan, T. R.; Hilgraf, R.; Sharpless, K. B.; Fokin, V. V. Polytriazoles as copper(I)-stabilizing ligands in catalysis. *Org. Lett.* **2004**, *6*, 2853−2855.
(67) Horne, W. S.; Yadav, M. K.; Stout, C. D.; Ghadiri, M. R. Heterocyclic peptide backbone modifications in an alpha-helical coiled coil. *J. Am. Chem. Soc.* **2004**, *126*, 15366−15367.
(68) Shooter, G. K.; Magee, B.; Soos, M. A.; Francis, G. L.; Siddle, K.; Wallace, J. C. Insulin-like growth factor (IGF)-I A- and B-domain analogues with altered type 1 IGF and insulin receptor binding specificities. *J. Mol. Endocrinol.* **1996**, *17*, 237−246.
(69) Menting, J. G.; Whittaker, J.; Margetts, M. B.; Whittaker, L. J.; Kong, G. K. W.; Smith, B. J.; Watson, C. J.; Zakova, L.; Kletvikova, E.; Jiracek, J.; Chan, S. J.; Steiner, D. F.; Dodson, G. G.; Brzozowski, A. M.; Weiss, M. A.; Ward, C. W.; Lawrence, M. C. How insulin engages its primary binding site on the insulin receptor. *Nature* **2013**, *493*, 241−245.
(70) Menting, J. G.; Lawrence, C. F.; Kong, G. K. W.; Margetts, M. B.; Ward, C. W.; Lawrence, M. C. Structural congruency of ligand binding to the insulin and insulin/type 1 insulin-like growth factor hybrid receptors. *Structure* **2015**, *23*, 1271−1282.
(71) De Meyts, P. The structural basis of insulin and insulin-like growth factor-I receptor binding and negative co-operativity, and its relevance to mitogenic versus metabolic signalling. *Diabetologia* **1994**, *37*, S135−S148.
(72) Picha, J.; Buděšínský, M.; Machackova, K.; Collinsova, M.; Jiracek, J. Optimized syntheses of Fmoc azido amino acids for the preparation of azidopeptides. *J. Pept. Sci.* **2017**, *23*, 202−214.
(73) Sell, C.; Dumenil, G.; Deveaud, C.; Miura, M.; Coppola, D.; Deangelis, T.; Rubin, R.; Efstratiadis, A.; Baserga, R. Effect of a null mutation of the insulin-like growth-factor-I receptor gene on growth and transformation of mouse embryo fibroblasts. *Mol. Cell. Biol.* **1994**, *14*, 3604−3612.
(74) Slaaby, R.; Andersen, A. S.; Brandt, J. IGF-I binding to the IGF-I receptor is affected by contaminants in commercial BSA: The contaminants are proteins with IGF-I binding properties. *Growth Horm. IGF Res.* **2008**, *18*, 267−274.
(75) Aguilar, H. N.; Zielnik, B.; Tracey, C. N.; Mitchell, B. F. Quantification of rapid myosin regulatory light chain phosphorylation

DOI: 10.1021/acs.jmedchem.7b01331
J. Med. Chem. 2017, 60, 10105−10117

using high-throughput in-cell western assays: comparison to western immunoblots. *PLoS One* **2010**, *5*, e9965.

DOI: 10.1021/acs.jmedchem.7b01331
J. Med. Chem. 2017, 60, 10105−10117